Myelin Basic Protein Associates with AβPP, Aβ$_{1-42}$, and Amyloid Plaques in Cortex of Alzheimer's Disease Brain

Xinhua Zhan[a,*], Glen C. Jickling[a], Bradley P. Ander[a], Boryana Stamova[a], DaZhi Liu[a], Patricia F. Kao[b,c], Mariko A. Zelin[b,c], Lee-Way Jin[b,c], Charles DeCarli[a,b] and Frank R. Sharp[a]

[a]*Department of Neurology, MIND Institute, University of California at Davis, Sacramento, CA, USA*
[b]*Alzheimer's Disease Center, University of California at Davis, Sacramento, CA, USA*
[c]*Department of Pathology, University of California at Davis, Sacramento, CA, USA*

Abstract. The goal of this study was to show that myelin and axons in cortical gray matter are damaged in Alzheimer's disease (AD) brain. Superior temporal gyrus gray matter of AD patients (9 male, 14 female) was compared to cognitively normal controls (8 male, 7 female). Myelin basic protein (MBP) and a degraded myelin basic protein complex (dMBP) were quantified by Western blot. Brain sections were immunostained for MBP, dMBP, axonal neurofilament protein (NF), autophagy marker microtubule-associated proteins 1A/B light chain 3B precursor (LC3B), amyloid-β protein precursor (AβPP), and amyloid markers amyloid β$_{1-42}$ (Aβ$_{1-42}$) and FSB. Co-immunoprecipitation and mass spectroscopy evaluated interaction of AβPP/Aβ$_{1-42}$ with MBP/dMBP. Evidence of axonal injury in AD cortex included appearance of AβPP in NF stained axons, and NF at margins of amyloid plaques. Evidence of myelin injury in AD cortex included (1) increased dMBP in AD gray matter compared to control ($p < 0.001$); (2) dMBP in AD neurons; and (3) increased LC3B that co-localized with MBP. Evidence of interaction of AβPP/Aβ$_{1-42}$ with myelin or axonal components included (1) greater binding of dMBP with AβPP in AD brain; (2) MBP at the margins of amyloid plaques; (3) dMBP co-localized with Aβ$_{1-42}$ in the core of amyloid plaques in AD brains; and (4) interactions between Aβ$_{1-42}$ and MBP/dMBP by co-immunoprecipitation and mass spectrometry. We conclude that damaged axons may be a source of AβPP. dMBP, MBP, and NF associate with amyloid plaques and dMBP associates with AβPP and Aβ$_{1-42}$. These molecules could be involved in formation of amyloid plaques.

Keywords: Alzheimer's disease, amyloid-β, amyloid-β protein precursor, autophagy, axon damage, degraded myelin basic protein, myelin basic protein

INTRODUCTION

Alzheimer's disease (AD) is characterized by progressive memory and cognitive impairment associated with extracellular senile plaques and intracellular neurofibrillary tangles in the brain [1]. Although cognitive dysfunction in AD correlates with amyloid-β (Aβ) and tau pathology, the roles of Aβ and tau in the pathogenesis of AD are still being elucidated. Additional cellular abnormalities may also contribute to AD including disruption of cerebral white matter.

In his original description Alzheimer noted intracellular lipid deposits in cerebral white matter [2, 3]. The role of lipids in AD received additional support when an apolipoprotein E4 (ApoE4) variant was associated with late-onset sporadic AD [4, 5]. Recently, other myelin lipid alterations have been reported in AD [6–9] further supporting the possibility that myelin injury is involved in the pathogenesis of AD [6, 9–21]. Indeed, initial amyloid deposits develop in poorly myelinated gray matter areas [22, 23] and myelin breakdown is

*Correspondence to: Xinhua Zhan, MD, PhD, University of California at Davis, M.I.N.D. Institute – Room 2415, 2805 50th Street, Sacramento, CA 95817, USA. Tel.: +1 916 703 0449; Fax: +1 916 703 0369; E-mail: xzhan@ucdavis.edu.

observed at the earliest stages of AD pathology [9, 10, 12, 15, 21]. Imaging studies also demonstrate greater loss of myelin integrity in patients with AD compared to normal aging and this loss precedes the onset of cognitive impairment [10].

Based on these findings, we hypothesized that axon and myelin damage occur in AD gray matter, and that accumulation of myelin breakdown products might associate with amyloid plaques in late-onset sporadic AD brains. We find evidence of axonal damage in AD brain associated with appearance of AβPP in fragmented axons. An antibody that detects injured white matter showed that a degraded myelin basic protein complex (dMBP) was increased in AD gray matter, myelin basic protein (MBP) is present at the margins of amyloid plaques, and dMBP co-localizes with Aβ_{1-42} in the core of amyloid plaques. The data suggest that axon damage leads to AβPP accumulation at sites of damage which might serve as a source of Aβ in AD plaques. The myelin damage could be the result of toxic effects of amyloid or secondary to the axonal injury and be deposited in already formed plaques. Alternatively, though intact MBP is reported to bind and degrade Aβ [24], dMBP may only bind Aβ but not degrade it and therefore could contribute to formation of amyloid plaques in AD brain.

MATERIALS AND METHODS

Brain samples

The Institutional Review Board approved the study, and informed consent was obtained for all study participants. The diagnosis of AD was made by board certified neurologists and confirmed by certified neuropathologists. AD was rated using CERAD criteria [25] and Braak stage [22]. A total of 38 brains including 23 AD and 15 controls were studied. Brain tissue was provided by the Alzheimer's Disease Center at University of California Davis. The superior temporal gyrus was studied since this region is commonly involved in AD. Controls were age-matched individuals without cognitive deficits as determined by neuropsychological testing at the UCD Alzheimer Disease Center. Brains used for immunostaining included 10 AD and 5 controls. For immunostaining, brains were fixed in formalin solution. Blocks of tissues were removed and embedded in paraffin and coronal sections used for immunostaining. Brains used for Western blot analysis included 13 AD and 10 controls. Fresh frozen tissues were used for Western blot analysis.

Immunohistochemistry

After paraffin removal and hydration of tissue sections through xylenes and a graded alcohol series, brain sections were treated with antigen retrieval buffer (25 mM Tris, 3 mM KCL, 140 mM NaCl, 1 mM EDTA, and 0.05% Tween 20 in distilled water) for 20 min at 95°C. Sections were then treated with 3% H_2O_2 in PBS for 20 min to quench endogenous peroxidase activity. After blocking nonspecific sites with blocking buffer (2% horse serum, 1% BSA, and 0.3% Triton 100 in 0.1 M PBS), sections were incubated with primary antibodies overnight at 4°C. The secondary antibody was a biotinylated goat anti-mouse or goat anti-rabbit IgG (1:200 dilution, Vector Labs, USA) depending on the primary antibody species. The antibody complex was detected using the peroxidase ABC system with diaminobenzidine (DAB) as the substrate according to the manufacturer's instructions (Vector Labs). Primary antibody was omitted to assess non-specific staining of the secondary antibody.

Immunofluorescence

After paraffin removal and antigen retrieval as above, brain sections were treated for autofluorescence using Autofluorescence Eliminator Reagent (Millipore, USA) according to the manufacturer's instructions. After blocking nonspecific sites, sections were incubated with primary antibodies. Goat anti-mouse or goat anti-rabbit Alexa Fluor® 488 or 594 conjugated antibodies (Invitrogen, USA) were used for secondary antibodies depending on the primary antibody species. Slides were cover slipped with a medium containing DAPI (Vector Labs, USA).

Antibodies used for immunocytochemistry

Primary antibodies were diluted at 1:500 unless otherwise stated. Primary antibodies included: mouse monoclonal antibodies against MBP (Millipore, MBP382, epitope 129–138, 1:10 dilution), AβPP (Millipore, MAB348, epitope 66–81, 1:2,000 dilution), Aβ_{1-16} (Covance), Aβ_{17-24} (Covance), Aβ_{1-42} (Covance), and neurofilament (NF) (Millipore, MAB5254, Anti-Neurofilament 160 kDa Antibody, 1:1,000 dilution); and rabbit polyclonal antibodies that detected a degraded myelin basic protein complex we call dMBP (Millipore, AB5864, specificity: recognizes MBP in demyelinated areas of brain, MBP epitopes 69–86) and microtubule-associated proteins 1A/B light chain 3B precursor (LC3b, 3868S, Cell Signaling).

FSB staining

FSB (Millipore) ((E, E)-1-fluoro-2,5-bis (3-hydroxycarbonyl-4-hydroxy) styrylbenzene), a derivative of Congo red, was used to stain amyloid plaques as described previously [26]. After immunostaining, sections were immersed in $1 \mu M$ FSB for 20 min, then rinsed in PBS and examined with fluorescence microscopy.

Slides for immunohistochemistry, immunofluorescence, and FSB staining were examined under a Nikon Eclipse E600 microscope (Nikon Corp, Japan). Images were captured using SPOT 4.6 imaging software (Diagnostic Instruments Inc. San Francisco, CA). Fluorescent microscopy was conducted at excitation/emission wavelengths of 493/520 (for green fluorochrome Alexa 488) or 590/619 (for red fluorochrome Alexa 594) nm or 358/463 nm (for fluorochrome FSB or DAPI).

Western blot analysis

Brain tissue from the superior temporal gyrus gray matter was removed and frozen at $-70°C$. Frozen tissues were homogenized in ice-cold RIPA buffer containing a complete protease inhibitor mixture (Sigma). Homogenates were centrifuged at $14,000 \times g$ for 30 min at $4°C$. The protein in the supernatant was loaded ($25 \mu g$ each) onto lanes and separated on 10% SDS polyacrylamide gels and transferred to nitrocellulose. The membranes were probed overnight at $4°C$ with anti-MBP (1:2,000 dilutions) or anti-dMBP (1:1,000 dilutions) antibody separately. Primary antibody was detected using horseradish peroxidase-conjugated anti-rabbit or anti-mouse IgG (Bio-Rad). The signal was detected using the ECL chemiluminescent detection system (PIERS Inc.). Blots were imaged on the Fluorchem 8900 system (Alpha Innotech). β-actin was used as a loading control. The ratio of the intensity of MBP band or dMBP band to that of β-actin band was quantified with NIH Image J software. Band intensity was expressed relative to the intensity of the band in the control samples.

Protein co-immunoprecipitation

Protein–protein interactions were performed using co-immunoprecipitation (Co-IP) with specific dMBP, AβPP, or $Aβ_{1-42}$ antibodies. IP products from antibodies against dMBP, AβPP, or $Aβ_{1-42}$ were used to evaluate the protein–protein interactions between dMBP and AβPP/$Aβ_{1-42}$. In addition, the IP product from an antibody against $Aβ_{1-42}$ was used for mass spectrometry analysis [27] to determine the proteins that co-immunoprecipitated with $Aβ_{1-42}$ and therefore either bound directly or indirectly to $Aβ_{1-42}$. Twenty μl of rabbit polyclonal antibody specific for dMBP (recognizes epitopes 69–86) or mouse monoclonal antibody against AβPP or $Aβ_{1-42}$ was added directly to $100 \mu g$ of the protein samples of control and AD brains. The mixture of antibody and proteins was incubated with rotation at $4°C$ for 4 h. Then $20 \mu l$ of protein G sepharose beads was added to the mixture and incubated with rotation at $4°C$ overnight. The mixture was then centrifuged at $600 \times g$ at $4°C$ for 30 s. After centrifugation, the supernatant was removed and the beads were washed with RIPA buffer five times. After washing, the precipitated proteins were eluted with loading buffer and analyzed by Western blotting. A control was carried out using normal rabbit or mouse IgG that replaced the specific antibodies.

LC-MS\MS analysis

IP was performed using mouse monoclonal antibody against $Aβ_{1-42}$ from a sample of superior temporal gyrus of AD brain. Immunoprecipitated proteins were digested first by washing the beads five times with 50 mM ammonium bicarbonate (AMBIC). Trypsin was then added in a ratio of 1:30 (enzyme:protein) and samples were digested overnight at room temperature. The next day, the IP beads were pelleted by centrifugation and the supernatant was collected. TCEP (Thermo Scientific) was added to a final concentration of 10 mM to reduce cysteine bonds, and samples were incubated for 10 min at $90°C$. Reduced cysteine residues were then alkylated for 1 h at room temperature with the addition of iodoacetamide (IAA) to a final concentration of 15 mM. 5 mM of dithiothreitol was added to quench the IAA reaction. Samples were then cleaned up by solid phase extraction using HyperSep Tips (Thermo Scientific).

LC separation was done on a Proxeon Easy-nLC II HPLC (Thermo Scientific) with a Proxeon nanospray source. The digested peptides were reconstituted in 2% acetonitrile/0.1% trifluoroacetic acid and $10 \mu l$ of each sample was loaded onto a $100 \mu m \times 25$ mm Magic C18 100Å 5U reverse phase trap where they were desalted online before being separated on a $75 \mu m \times 150$ mm Magic C18 200Å 3U reverse phase column. Peptides were eluted using a gradient of 0.1% formic acid (A) and 100% acetonitrile (B) with a flow rate of 300 nL/min. A 60-min gradient was run with 5% to 35% B over 45 min, 35% to 80%

B over 5 min, 80% B for 1 min, 80% to 5% B over 1 min, and finally held at 5% B for 8 min.

Mass spectra were collected on an Orbitrap Q Exactive mass spectrometer (Thermo Fisher Scientific) in a data-dependent mode with one MS precursor scan followed by 15 MS/MS scans. A dynamic exclusion of 5 s was used. MS spectra were acquired with a resolution of 70,000 and a target of 1×10^6 ions or a maximum injection time of 20 ms. MS/MS spectra were acquired with a resolution of 17,500 and a target of 5×10^4 ions or a maximum injection time of 250 ms. Peptide fragmentation was performed using higher-energy collision dissociation with a normalized collision energy value of 27. Unassigned charge states as well as +1 and ions >+5 were excluded from MS/MS fragmentation. The methods follow standard protocols [28].

MS data analysis

Tandem mass spectra were extracted and charge states were deconvoluted and deisotoped. All MS/MS samples were analyzed using X! Tandem (The GPM, http://thegpm.org/; version CYCLONE (2013.02.01.1)). X! Tandem was set up to search the Uniprot Human reference database (May, 2013; 20252 entries) plus an equal number of reverse sequences and 60 common laboratory contaminant proteins, using the digestion enzyme trypsin. X! Tandem was searched with a fragment ion mass tolerance of 20 PPM and a parent ion tolerance of 20 PPM. Carbamidomethyl of cysteine was specified in X! Tandem as a fixed modification. Glu->pyro-Glu of the N-terminus, ammonia-loss of the N-terminus, gln->pyro-Glu of the N-terminus, oxidation of proline, dioxidation of methionine and tryptophan and acetyl of the N-terminus were specified in X! Tandem as variable modifications.

Scaffold (Scaffold_4.3.2, Proteome Software Inc., Portland, OR) was used to validate MS/MS based peptide and protein identifications. Peptide identifications were accepted if they could be established at greater than 95.0% probability by the Scaffold Local FDR algorithm. Protein identifications were accepted if they could be established at greater than 20.0% probability to achieve an FDR less than 5.0% and contained at least 1 identified peptide. Protein probabilities were assigned by the Protein Prophet algorithm [28]. Proteins that contained similar peptides and could not be differentiated based on MS/MS analysis alone were grouped to satisfy the principles of parsimony. Proteins sharing significant peptide evidence were grouped into clusters. Using these parameters, a false discovery rate

was calculated at <1% on the peptide level and <5% on the protein level for samples searched against the Uniprot Human reference database.

Statistical analysis

Differences between groups were analyzed using a Student *t*-test (continuous), Wilcoxon-Mann Whitney test (ordinal) or Fisher Exact test (categorical). A *P* value ≤0.05 was considered significant.

RESULTS

Patient characteristics

Characteristics of the 23 AD and 15 control patients are shown in Supplementary Table 1. There were no significant differences in gender or age for AD (79.8 ± 1.9) compared to controls (80.5 ± 1.2). The postmortem interval (PMI) for the AD patients was 13.3 ± 3.5 h and the PMI for the control subjects was 16.8 ± 4.4 h, which were not significantly different ($p = 0.27$). The median Braak and Braak stage [22] was 6 in the AD patients, and 2 in the cognitively normal controls which were significantly different ($p < 0.001$). There were significant differences of CERAD plaque scores in AD compared to control patients, with 20/23 AD patients and 0/15 controls having CERAD plaque scores of C (Supplementary Table 1). Most AD cases had severe, late stage pathology.

Myelin injury occurred in AD and aged control brains

In preliminary studies we identified the molecular weight of MBP ($\sim$19 kDa) and the degraded myelin basic protein complex we call dMBP ($\sim$37 kDa) in two separate experiments (Supplementary Figure 1). To better compare MBP and dMBP levels, we performed double staining of MBP and dMBP in the same membrane (Fig. 1). Using the intact MBP antibody, we identified a protein with a 19 kDa molecular weight by Western blot analysis in both control and AD brains (Fig. 1A, Supplementary Figure 1). The overall expression of 19 kDa MBP is significantly increased in AD brains compared to controls (Fig. 1A, B, $p < 0.05$). Of interest, there was one AD case (Fig. 1A, upper panel, black arrow, PMI = 3.0 h) and one control case (Fig. 1A, lower panel, black arrow, PMI = 10.0 h) that showed a marked decrease of the 19 kDa MBP band (see below). The PMI in these two subjects (3.0 h in the AD subject and 10.0 h in control subject, respectively)
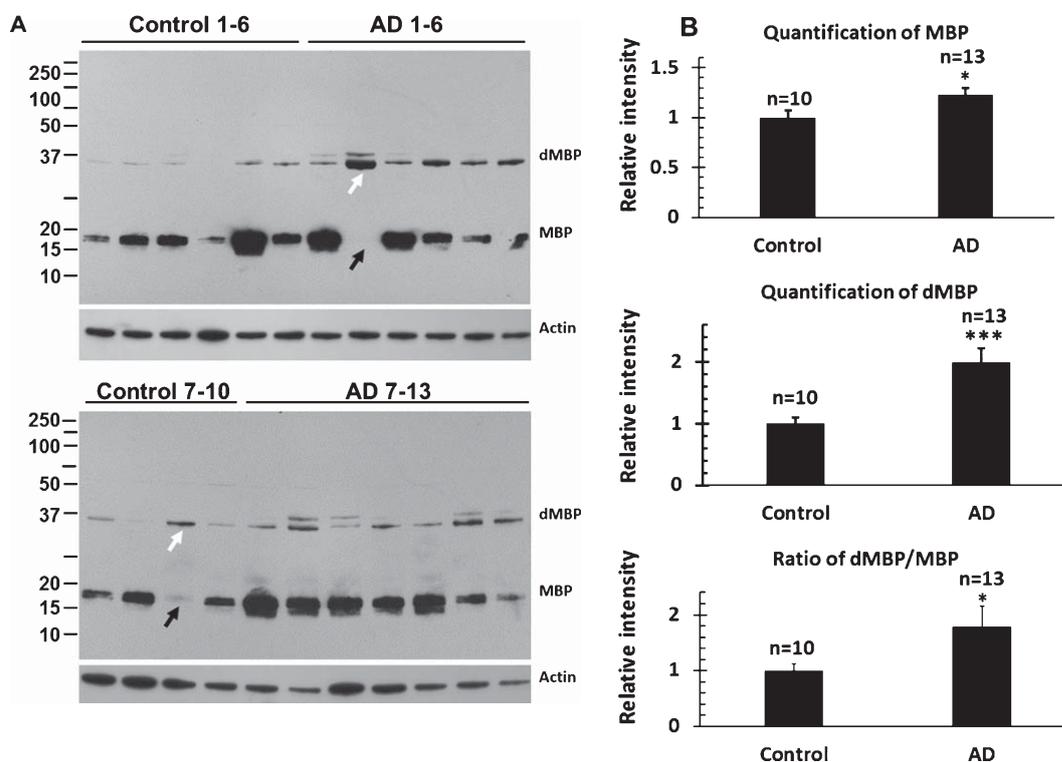
Fig. 1. Western blot analysis of MBP and dMBP in control ($n = 10$) and AD ($n = 13$) brains. Both intact MBP ($\sim$19 kDa) and degraded MBP ($\sim$37 kDa) were detected in control and AD brains. Note that intact MBP was markedly decreased in one AD case (A, upper panel, black arrow). In the same case, dMBP was markedly increased (A, upper panel, white arrow). Similarly, intact MBP was markedly decreased in one out of 10 control brains (A, lower panel, black arrow). In the same case, dMBP was markedly increased (A, lower panel, white arrow). The overall expression of MBP in AD was significantly increased compared to control (B, upper panel). The dMBP levels in AD were significantly increased compared to control as well (B, middle panel). The ratio of dMBP over MBP was significantly higher in AD compared to control (B, lower panel). MBP, myelin basic protein; dMBP, degraded myelin basic protein complex; AD, Alzheimer's disease. $^*p < 0.05$ versus control, $^{***}p < 0.001$ versus control. Error bars are standard errors of the mean.

were shorter than the average PMI in the groups they belonged to (AD: 13.3 ± 3.5 h; control: 16.8 ± 4.4 h). This suggested that the PMI was not a main factor contributing to differences of MBP and dMBP in these cases.

Using an antibody that has been shown to specifically detect damaged white matter by immunocytochemistry in human AD brain [29, 30] (see discussion), we identified a $\sim$37 kDa molecular weight band by Western blot analysis in both control and AD brains (Fig. 1A). An additional protein band at $\sim$42 kDa was found mostly in AD brains (Fig. 1A). For the purposes of this study, we call the $\sim$37 kDa and $\sim$42 kDa bands degraded myelin basic protein complexes and abbreviate this as dMBP. It is important to emphasize that the antibody to dMBP detected bands at $\sim$37 kDa or $\sim$42 kDa but not at $\sim$19 kDa; whereas the antibody to intact MBP only detected bands around 19 kDa, but not at $\sim$37 kDa or $\sim$42 kDa (Supple-

mentary Figure 1). Thus, this is why we believe the dMBP antibody is detecting MBP complexes, where degraded MBP (or less likely intact MBP) is bound to other proteins (see discussion).

The blots showed the $\sim$37 kDa dMBP band was much more prominent in AD brains than in controls (Fig. 1A), and this was confirmed by quantification of the bands (Fig. 1B, middle panel, $^{***}p < 0.001$). Additionally, the ratio of band intensities of dMBP over MBP is much larger in AD compared to control (Fig. 1B, lower panel, $^*p < 0.05$).

Some controls did not have the $\sim$37 kDa dMBP band (Fig. 1A). The $\sim$42 kDa dMBP band was observed in most AD brains and several controls, though not all AD cases had the $\sim$42 kDa dMBP band (Fig. 1A). It is notable that the AD case with little intact MBP (black arrow, Fig. 1A, upper panel) had a large amount of the $\sim$37 kDa dMBP and $\sim$42 kDa dMBP bands (white arrow, Fig. 1A, upper panel). In addition, the control

case with little intact MBP (black arrow, Fig. 1A, lower panel) had a large amount of the ∼37 kDa dMBP band (white arrow, Fig. 1A, lower panel). These data support the possibility that loss of intact MBP led to increased levels of dMBP in these two subjects. As noted above, PMI did not correlate with this break down.

Accumulation of MBP in pyramidal neurons of AD brains

We next sought to localize intact MBP and dMBP in the cortical gray matter samples. Using the antibody that detected intact MBP, MBP stained myelin sheaths were apparent throughout the cortex of control subjects (Fig. 2A1). In contrast, only sparsely stained MBP myelin sheaths were found in cortex of AD patients (Fig. 2B1). In addition, there was staining of intact MBP in the cell bodies of neurons in AD cortex (Fig. 2B1 and 2B2, arrows), which was not observed in control cortex (Fig. 2A1, 2A2).

Using the antibody to dMBP, we observed myelin sheaths of variable size in the AD cortex (Fig. 2D1, black arrows) with little or no staining seen in control brains (Fig. 2C1). There was also a suggestion that dMBP was increased in the cytoplasm and nuclei of some neurons in cortex in AD brain (Fig. 2D2) compared to controls (Fig. 2C2).

Since the dMBP data suggested damage to myelin sheaths, we examined the axonal protein NF. NF stained axons were prominent in control brain (Fig. 3A1) with less discrete NF axonal staining in AD brain (Fig. 3B1). In addition, there appeared to be an increase in NF staining in AD neurons in cytoplasm and perhaps even nuclei (Fig. 3B1, 3B2) compared to control cortex (Fig. 3A1, 3A2). These could represent neurofibrillary tangles or pre-tangles since tau was not examined in this study.

Autophagy of myelin sheaths in AD brains

The above data raised the possibility that the damaged axons and myelin sheaths could be degraded via autophagy [31, 32]. Therefore, we compared localization of MBP and the autophagy marker LC3B in control (Supplementary Figure 2A) and AD brains (Supplementary Figure 2B). There was little expression of the LC3B protein in control cortex (Supplementary Figure 2A2). In contrast, the LC3B protein was expressed in AD cortex, with the LC3B protein (Supplementary Figure 2B2) and MBP protein (Supplementary Figure 2B1) being co-localized (Supplementary Figure 2B3).

AβPP staining in damaged axons in AD brains

Fragmentation of axons occurred in the AD brain as indicated by discontinuous staining of the axonal marker NF in the axons (Fig. 4B1, white arrows). In addition, immunostaining for AβPP appeared to be associated with fragmented axons in AD brain (Fig. 4B2) since AβPP co-localized with axonal NF staining (Fig. 4B3). In control brains NF stained axons were observed (Fig. 4A1) though there was no AβPP staining observed in these axons (Fig. 4A2, 4A3).

Molecules associated with amyloid plaques in AD brains

We next examined the relationship of the above molecules with amyloid plaques in AD brain. Staining for intact MBP showed multifocal MBP staining (yellow arrows, Fig. 5A) at the margins of amyloid plaques (outlined with red arrows, Fig. 5A) but not in the core of the plaque (blue arrow, Fig. 5A). Some plaques had aggregates of NF stained axons/neurons (Fig. 5B, red arrow). Most plaques demonstrated $A\beta_{1-42}$ staining of the plaque core (Fig. 5C, blue arrow). Of interest $A\beta_{1-42}$ did not stain in neurons adjacent to plaques (Fig. 5C, black arrows). In contrast, $A\beta_{1-16}$ (Fig. 5D), $A\beta_{17-24}$ (Fig. 5E), and AβPP (Fig. 5F) are identified both in amyloid plaques (Fig. 5D, 5E, and 5F, red arrows) and neurons (Fig. 5D, 5E, and 5F, black arrows) in AD brain.

dMBP, MBP, and NF associate with amyloid plaques

Given the above data we directly examined the relationships between amyloid plaques (stained with FSB [26] or $A\beta_{1-42}$) and MBP, dMBP, and NF in AD brain (Fig. 6). Some of the MBP aggregates in AD cortex (Fig. 6A2) were found within FSB stained plaques (Fig. 6A1, yellow arrows) whereas the majority were adjacent to FSB stained plaques (Fig. 6A1 and 6A3, white arrow). The NF stained aggregates (Fig. 6B2, white arrows) were also located at the periphery of the FSB stained amyloid plaques (Fig. 6B1, white arrows) with the NF staining generally not co-localizing with the FSB stained plaques (Fig. 6B3, white arrows). In contrast, we found that some foci of dMBP in AD cortex (Fig. 6C2, white arrows) occurred in association with $A\beta_{1-42}$ aggregates (Fig. 6C1, arrows) and that the dMBP and $A\beta_{1-42}$ were co-localized (Fig. 6C3, arrows).
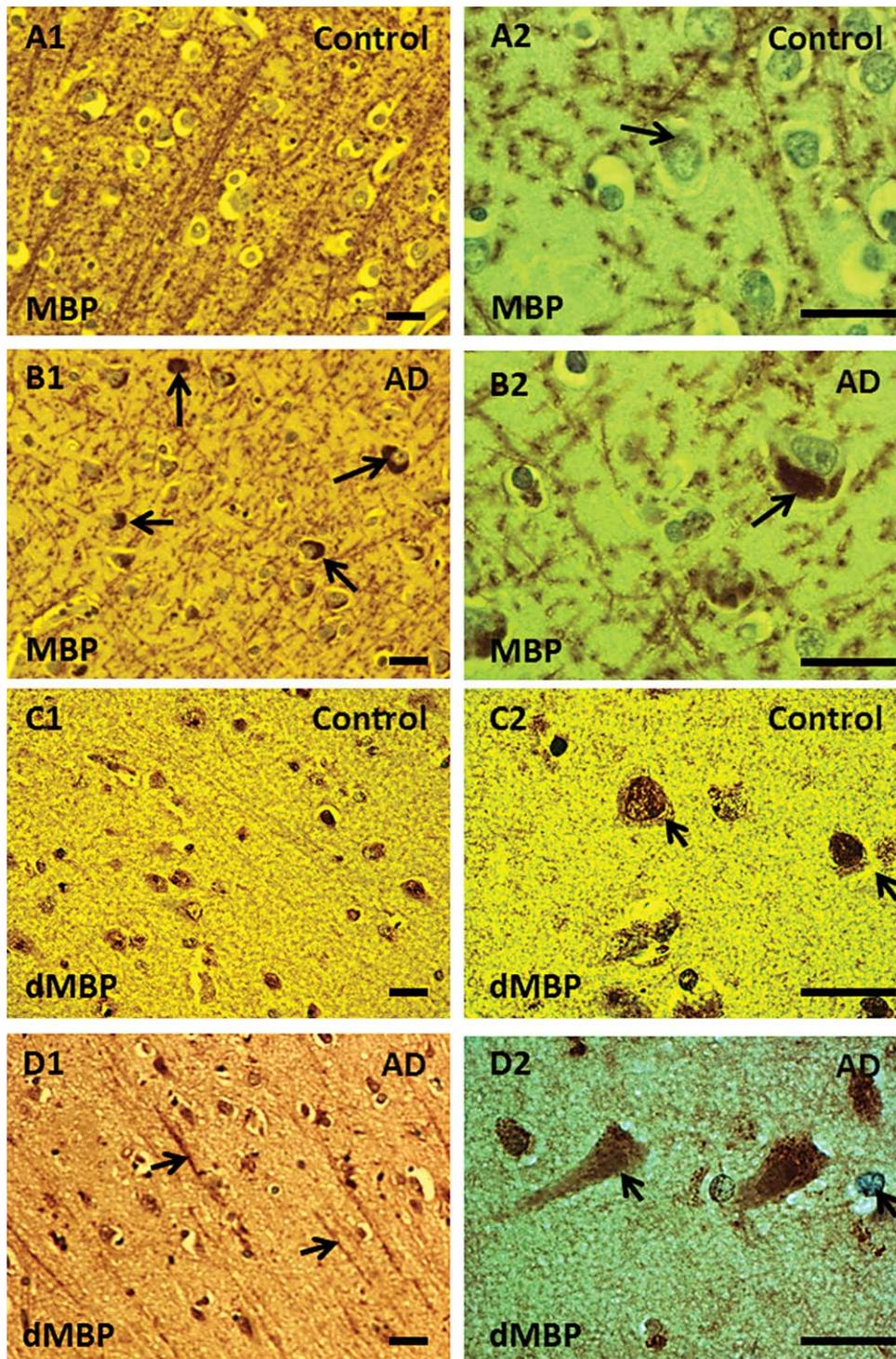
Fig. 2. Immunohistochemistry of MBP and dMBP in the cortex of control and AD brains. In controls, MBP was predominantly stained in the myelin sheaths of cortex (A1). In contrast, soma of the pyramidal neurons showed accumulation of intensively stained MBP (B1 and B2, arrows) in AD brains compared to controls (A2, arrow). Using an antibody specifically against degraded MBP, we detected degraded myelin protein in the giant myelin sheaths (D1, arrows), soma and nuclei (D2, arrows) of pyramidal neurons of AD brains. In controls, dMBP was also detected in the nuclei of the pyramidal neurons (C1 and C2). Brown, positive staining; MBP, myelin basic protein; dMBP, degraded myelin basic protein complex; AD, Alzheimer's disease. Bar = 25 μm.
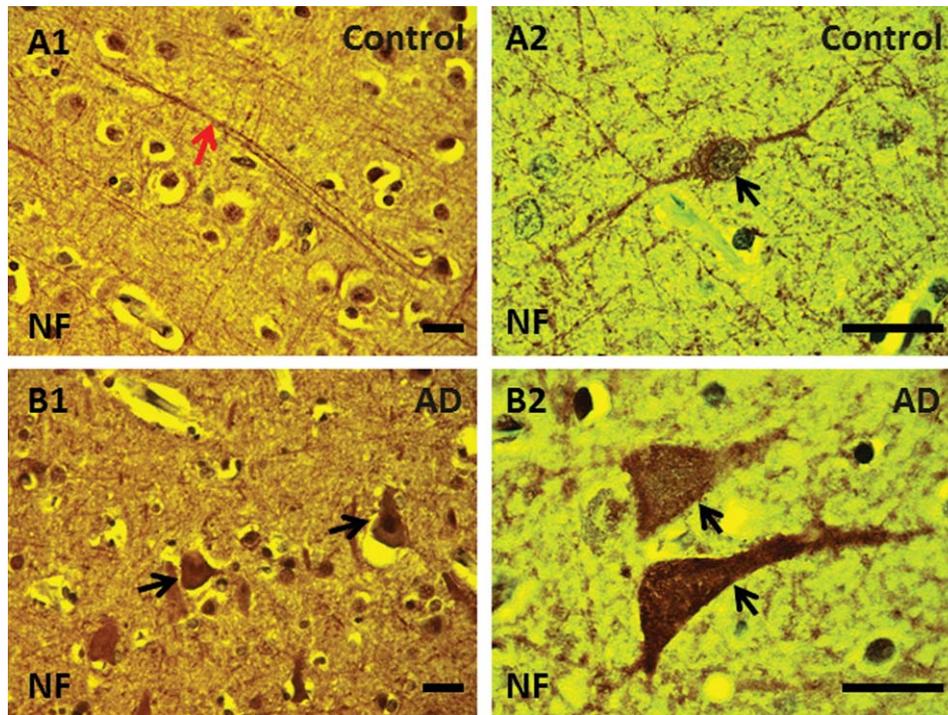
Fig. 3. Immunohistochemistry of NF in the cortex of control and AD brains. In controls, NF was stained in axons (A1 and A2, arrows) of neurons. NF was also stained in the soma of the pyramidal neurons (B1 and B2, arrows) of AD brains. In addition, the proximal portions of axons were thickened in the AD brain (B2). Brown, positive staining; NF, neurofilament; AD, Alzheimer's disease. Bar = 25 μm.
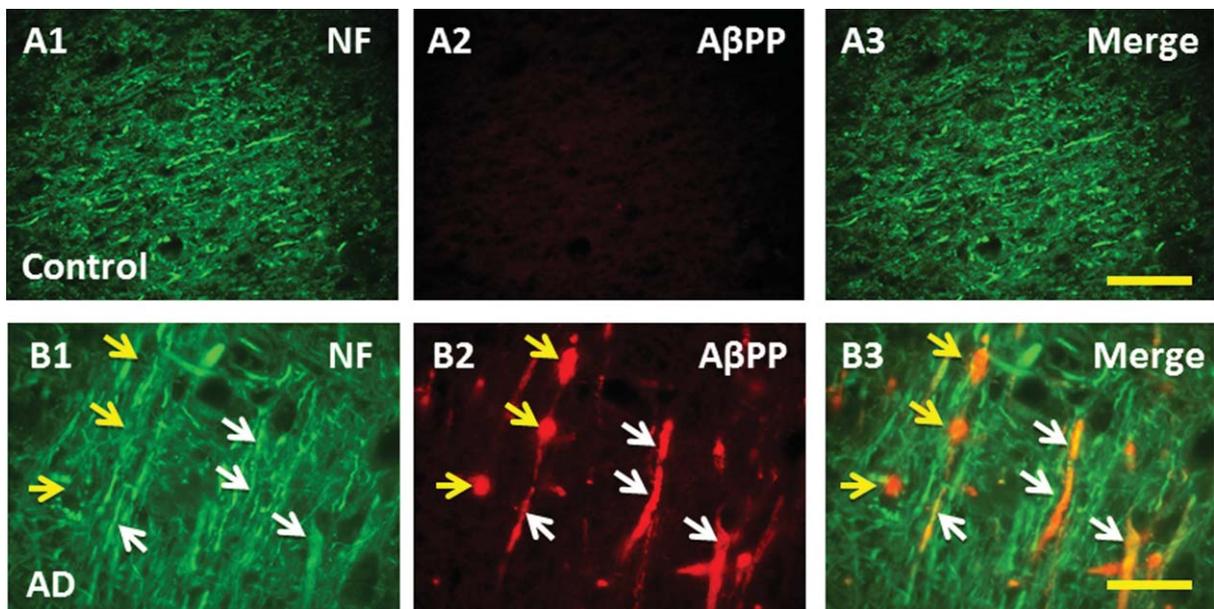

Fig. 4. Axonal injury associated with AβPP staining in AD brains. Axonal fragmentation was observed (B1, white arrows) in AD brain by immunofluorescence staining of an axonal marker, NF. AβPP was associated with these fragmented axons (B2 and B3, white arrows). In the areas where axonal fragmentation was severe or large areas of axons were lost (B1, yellow arrows), AβPP aggregates were observed (B2 and B3, yellow arrows). In control, NF was localized in axons or bundles of axons (A1) that did not stain for AβPP (A2 and A3). NF, neurofilament; AβPP, amyloid-β protein precursor; AD, Alzheimer's disease. Bar = 25 μm.
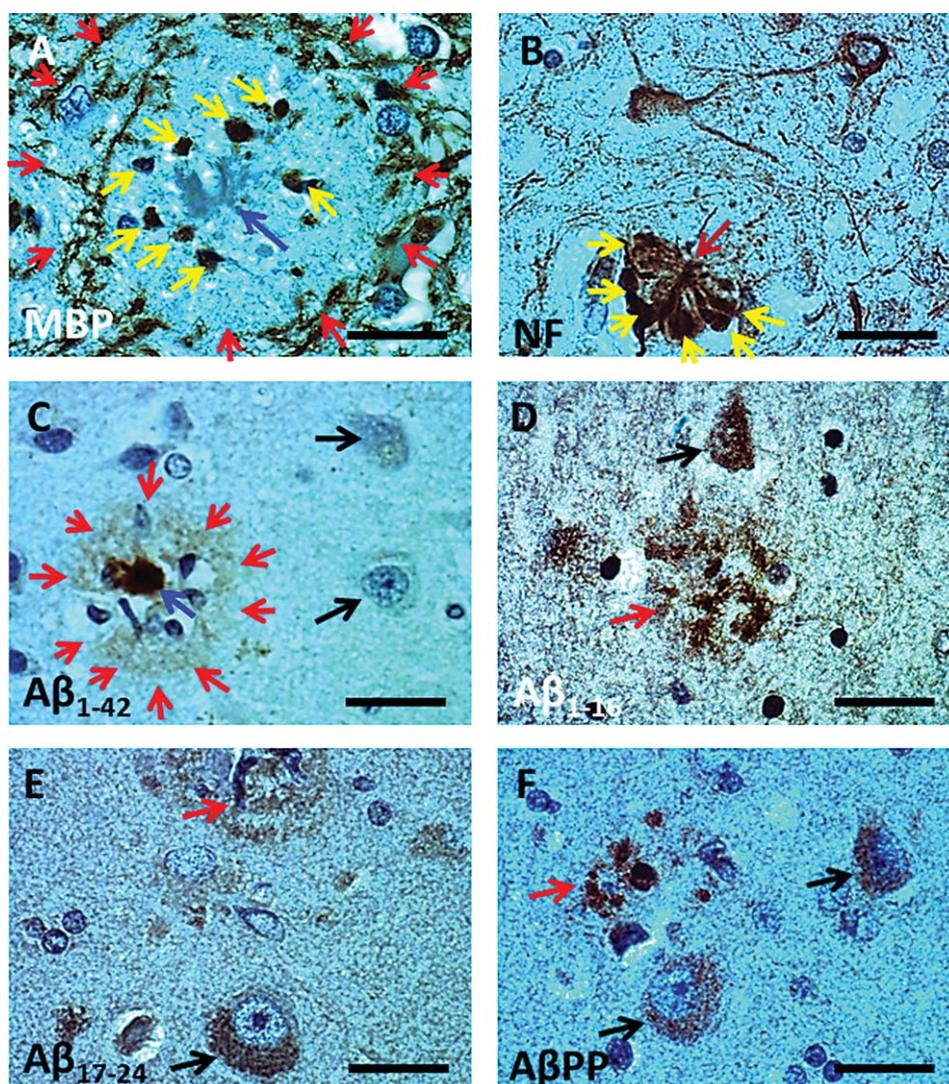
Fig. 5. Immunostaining of myelin/axonal aggregates and amyloid aggregates in AD brains. Myelin aggregates (A, yellow arrows) were observed in plaque-like structures (A, blue arrow surrounded by red arrows). MBP aggregates were localized in the halo (A, surrounded by red arrows), but not the core (A, blue arrow) of the plaque. Using the axonal marker, NF, we detected axonal aggregates (B, red arrow). The axons were tangles in the center while their somata orientated to the periphery (B, yellow arrows). $A\beta_{1-42}$ was not stained in the pyramidal neurons (C, black arrows), but $A\beta_{1-42}$ did stain in the core (C, blue arrow surrounded by red arrows) of the plaque. In addition, short fragments of $A\beta$ such as $A\beta_{1-16}$ (D) and $A\beta_{17-24}$ (E), as well as $A\beta PP$ (F) were identified both in the plaques (D, E, F, red arrows) and pyramidal neurons (D, E, F, black arrows). Brown, positive staining; MBP, myelin basic protein; NF, neurofilament; $A\beta PP$, amyloid-β protein precursor; $A\beta$, amyloid-β; AD, Alzheimer's disease. Bar = 25 μm.

Interaction of dMBP with AβPP or Aβ_{1-42} in AD and aged control brains

Immunoprecipitation (IP) was performed using the dMBP antibody (used in Fig. 1) in both AD ($n = 4$) and control ($n = 4$) brains. The IP product was immunoblotted with an AβPP antibody to demonstrate the interaction between AβPP and dMBP (Fig. 7). Two bands ($\sim$32 kDa and $\sim$27 kDa) were detected in both control and AD brains (Fig. 7A, upper band a, lower band b). The density of the two bands was generally greater in each AD brain compared to control brains (Fig. 7A). Quantification confirmed more protein in both bands in AD compared to control brains (Fig. 7B, $*p < 0.05$ for upper band a, and $***p < 0.001$ for lower band b). We also performed controls in which immunoprecipitation was performed using IgG in PBS and in the control brain sample and AD brain sample followed
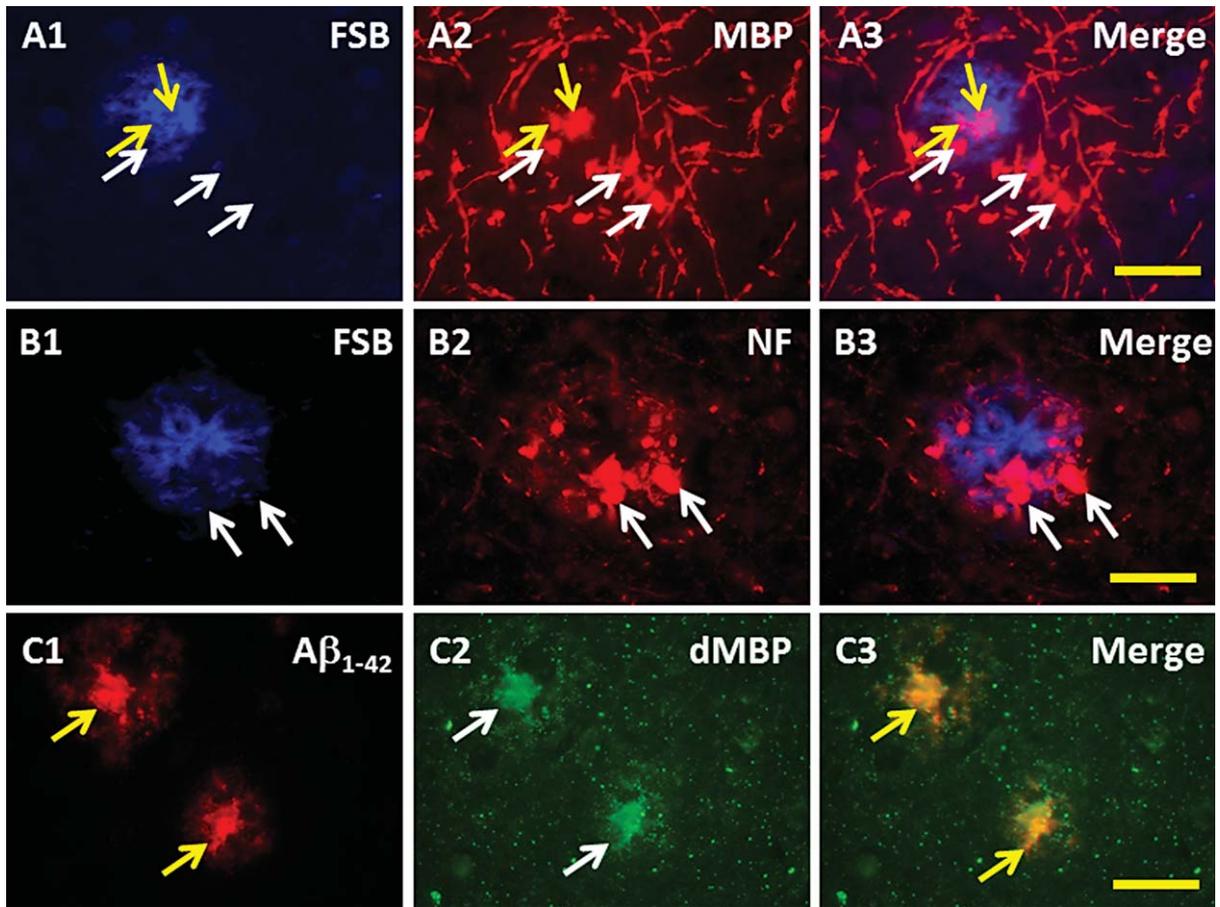
Fig. 6. Myelin/axonal aggregates in the amyloid plaques of AD brains. In FSB positive amyloid plaque (A1 and A3, yellow arrows), myelin aggregates (A2 and A3, arrows) were observed. Note that some MBP aggregates (A2 and A3, yellow arrows) are located in the amyloid plaque whereas other MBP aggregates (A2 and A3, white arrows) were adjacent, but not within the FSB$^+$ plaques. Similar NF$^+$ aggregates (B2 and B3, arrows) were observed in AD brain as well. These NF$^+$ aggregates were frequently located in the periphery of the FSB$^+$ amyloid plaque (B1, arrows). In addition, dMBP aggregates (C2, arrows) were identified in Aβ_{1-42}^+ plaques (C1 and C3, arrows) with dMBP and Aβ_{1-42} being co-localized (C3). MBP, myelin basic protein; dMBP, degraded myelin basic protein complex; Aβ, amyloid-β; NF, neurofilament; FSB, (E, E)-1-fluoro-2,5-bis (3-hydroxycarbonyl-4-hydroxy) styrylbenzene; AD, Alzheimer's disease. Bar = 25 μm.

by immunoblotting for AβPP (Fig. 7A, right side). This showed a ∼28 kDa band in control and AD brain, but not in PBS. These data are discussed below.

To further confirm the interaction of dMBP with AβPP/Aβ_{1-42}, we performed a reciprocal experiment of IP using anti-AβPP or anti-Aβ_{1-42} antibody (Fig. 7C). Immunoblots of the IP products with the dMBP antibody reveals the interaction of AβPP and Aβ_{1-42} with dMBP as indicated by detecting a ∼27 kDa protein in both AD and control brains (Fig. 7C, AβPP and Aβ_{1-42}). This ∼27 kDa protein appears to have the same molecular weight as the dMBP IP blotted with an antibody to AβPP in Fig. 7A, and thus this may be the same protein. That is, the same molecular weight species is observed whether AβPP or Aβ_{1-42} IP products are blotted with antibody to dMBP, or whether the

dMBP IP products are blotted with antibody to AβPP (Fig. 7A, band b).

Aβ_{1-42} associated proteins from LC-MS\MS analysis

MS analysis of the Aβ_{1-42} immunoprecipitation product showed that Aβ_{1-42} interacted with 186 proteins which include MBP, heat shock proteins, AβPP, ApoE, Tau, MAP1B, CNPase, neurofilament heavy polypeptide, and neurofilament light polypeptide (Table 1). Note that the percentage of total spectra of MBP (0.04%), neurofilament light polypeptide (0.04%), and neurofilament heavy polypeptide (0.02%) was higher than that of AβPP (0.01%) and tau (0.01%).
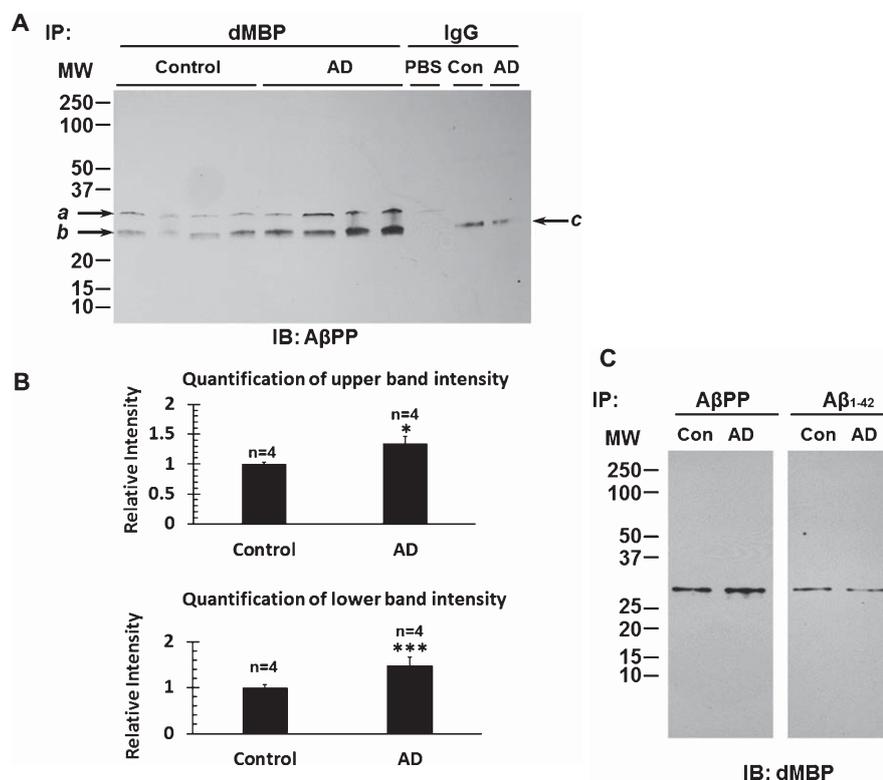
Fig. 7. Co-IP of dMBP, AβPP, or Aβ$_{1-42}$ in control and AD brains. A) Immunoprecipitation (IP) was performed using the dMBP antibody in both control and AD brains. Immunoblots of the IP product with the AβPP antibody reveals the interaction of dMBP with AβPP as indicated by detecting two bands (a and b) of protein in both AD and control brains (A). The molecular weight (MW) of the two bands was about 32 kDa (band a) and 27 kDa (band b), respectively. Using IgG as a negative control, we detected a protein with MW around ∼28 kDa (band c). It is likely that there is a specific binding of IgG with cleaved AβPP in aging brains since the binding was not detected when the brain sample was replaced by PBS (A). B) Quantification of the intensity of bands A and B. The intensity of the upper band A and lower band B was greater in AD compared to control brain (B). C) A reciprocal experiment of IP was performed using anti-AβPP or anti-Aβ$_{1-42}$ antibody to verify the findings in panel A. Immunoblots of the IP products with dMBP antibody reveals the interaction of AβPP or Aβ$_{1-42}$ with dMBP as indicated by detecting a protein in both AD and control brains (C). The MW of the protein is about 27 kDa. Comparing with IP result from panel A, it is likely that the protein with MW around 27 kDa is in the complex of dMBP-AβPP since this protein was detected in both IP products either with AβPP or dMBP. In addition, AβPP complexed with dMBP is likely containing Aβ$_{1-42}$ fragments since immunoblots with dMBP in IP product using Aβ$_{1-42}$ revealed same MW of protein as that in IP product using AβPP. AβPP, amyloid-β protein precursor; dMBP, degraded myelin basic protein complex; AD, Alzheimer's disease. *$p < 0.05$ versus control, ***$p < 0.001$ versus control. Error bars represent standard errors of the mean.

DISCUSSION

Axonal and myelin damage were detected in the superior temporal gyrus gray matter of AD brain. Evidence of axonal injury in AD cortex included localization of NF at margins of plaques and appearance of AβPP in injured axons. Evidence of myelin damage in AD cortex included localization of dMBP in the myelin sheaths, localization of MBP at margins of plaques, and co-localization of dMBP with Aβ$_{1-42}$ in plaques. These data could indicate that amyloid is toxic to axons and myelin, and proteins from these then associate with the amyloid plaques after they form. However, since recent studies show that MBP can bind and degrade Aβ [24, 33, 34], we postulate that dMBP can bind AβPP and Aβ$_{1-42}$ and possibly participate in the formation of amyloid plaques in AD brain. This hypothesis is supported by data that myelin damage can precede cognitive decline and amyloid plaque formation in humans [9, 10, 12, 35] and by data indicating myelin abnormalities precede amyloid and tau pathology in a transgenic AD mouse model [36].

Myelin damage in AD brains

Progressive loss of myelin integrity occurs in healthy adults after middle age in late myelinating regions such as the frontal lobe [10]. Loss of myelin staining has been demonstrated in aged animals as well [37, 38]. The loss of myelin with aging in humans is supported

Table 1
Identified proteins by mass spectrometry using the Aβ₄₂ Immunoprecipitation product from Alzheimer's disease temporal lobe cortex (partial listing of all of the proteins found)

Protein name	Protein molecular weight (Da)	Protein identification probability	Exclusive unique peptide count	Exclusive unique spectrum count	Total spectrum count	Percentage of total spectra	Percentage sequence coverage
Heat shock cognate 71 kDa protein OS = Homo sapiens GN = HSPA8 PE = 1 SV = 1	70,023.00	100.00%	2	2	7	0.06%	9.29%
Heat shock 70 kDa protein 1A/1B OS = Homo sapiens GN = HSPA1A PE = 1 SV = 5	70,054.00	100.00%	2	2	6	0.05%	9.05%
Myelin basic protein OS = Homo sapiens GN = MBP PE = 1 SV = 3	33,117.70	100.00%	3	3	5	0.04%	10.50%
Neurofilament light polypeptide OS = Homo sapiens GN = NEFL PE = 1 SV = 3	61,517.80	100.00%	2	2	5	0.04%	4.05%
Apolipoprotein E OS = Homo sapiens GN = APOE PE = 1 SV = 1	36,153.50	99.80%	1	1	2	0.02%	2.84%
Heat shock protein HSP 90-alpha OS = Homo sapiens GN = HSP90AA1 PE = 1 SV = 5	84,663.20	99.90%	0	0	2	0.02%	3.69%
Heat shock protein HSP 90-beta OS = Homo sapiens GN = HSP90AB1 PE = 1 SV = 4	83,267.30	99.90%	1	1	3	0.02%	5.11%
Neurofilament heavy polypeptide OS = Homo sapiens GN = NEFH PE = 1 SV = 4	112,480.10	82.50%	0	0	3	0.02%	0.88%
2′,3′-cyclic-nucleotide 3′-phosphodiesterase OS = Homo sapiens GN = CNP PE = 1 SV = 2	47,580.60	97.70%	1	1	1	0.01%	2.61%
Amyloid beta A4 protein OS = Homo sapiens GN = APP PE = 1 SV = 3	86,941.30	98.90%	1	1	1	0.01%	1.56%
Microtubule-associated protein 1B OS = Homo sapiens GN = MAP1B PE = 1 SV = 2	270,634.40	92.60%	1	1	1	0.01%	0.37%
Microtubule-associated protein tau OS = Homo sapiens GN = MAPT PE = 1 SV = 5	78,927.70	97.70%	1	1	1	0.01%	2.11%

by this study which shows that dMBP is detected in many but not all "normal aging" brains.

On top of the normal myelin loss with aging, a number of imaging and pathological studies have shown greater myelin loss and breakdown in AD compared to age-matched controls [10, 14, 16, 20, 39]. Specifically, there is less intact MBP in AD white matter compared to controls [40]. Our recent study using the same antibody to detect dMBP showed increased dMBP positive vesicles in the periventricular white matter of AD patients compared to age-matched controls [30]. These dMBP positive vesicles co-localized with PAS and were identified as corpora amylacea, which are increased in AD brain [41]. The current study extends our previous findings by showing that there is an increased amount of dMBP in gray matter of AD brains compared to age-matched cognitively normal controls. This finding is consistent with prior studies documenting myelin and lipid changes in the gray matter of AD brain [9, 19, 42, 43].

What the antibody to dMBP detects

The antibody to dMBP used in this study detects a ∼37 kDa band on Western blots that is larger than intact MBP (∼19 kDa). This rabbit polyclonal antibody (Millipore, AB5864) was raised to a synthetic peptide corresponding to amino acids 69–86 of the guinea pig MBP (http://www.millipore.com/catalogue/item/ab5864). The dMBP antibody has been used in at least five different studies for immunocytochemistry and shown not to recognize intact myelin but only damaged myelin in several different species. It has been used to detect damaged myelin in aging and AD human brain by others [29], and we have previously shown that it does not stain normal myelin but only stains damaged myelin and myelin vesicles in white matter of human AD and control brains [30]. Since the current study also shows that it does not stain normally myelinated axons in control or AD gray matter, this raises the question of what exactly does this antibody recognize?

Although the antibody to dMBP stains a protein at ∼37 kDa that is about double the size of intact MBP, the dMBP protein is unlikely a dimer of MBP since it is not detected by the antibody to intact MBP. Therefore, we postulate that the antibody to dMBP used in this study probably detects some fragment of MBP (degraded MBP/dMBP) which is complexed with one or more molecules. Our

data show that the dMBP detected by this antibody co-immunoprecipitates with AβPP. Though AβPP has a predicted molecular weight of 86.9, our AβPP antibody detects cleavage products of AβPP including cleaved AβPP molecules in the 20–30 kDa range (data not shown). Thus, one possibility is that the dMBP antibody detects a complex of dMBP and cleaved AβPP. Whatever portion of dMBP is recognized by the dMBP antibody in this study, it is not recognized by the antibody to intact MBP used in this study which was raised to intact bovine MBP and recognizes amino acids 129–138 of MBP (http://www.millipore.com/catalogue/item/mab382). Thus the dMBP antibody used in this study likely detects a degraded MBP protein that does not include amino acids 129–138, and this degraded MBP protein is complexed to at least one other protein, possibly cleaved AβPP. We use the dMBP abbreviation for this degraded myelin basic protein complex.

AD neurons contain MBP, dMBP, and NF

A pathological hallmark of AD neurons is the presence of aggregates of hyper-phosphorylated tau protein known as neurofibrillary tangles [44, 45] though tangles have been demonstrated in other neurological disorders [46, 47] including traumatic brain injury [48]. Cognitive impairment in AD correlates with the extent of neurofibrillary tangles [49]. This study demonstrates additional abnormal axonal and myelin proteins in AD neuronal cell bodies including NF, MBP, and dMBP. These could be transported into cell bodies from adjacent injured axons, or might represent abnormal accumulations of these proteins in neurons with injured axons. Neuronal intracellular MBP often occurred in areas where MBP disappeared from the axons, which suggests that neuronal MBP may be from myelin sheaths of the injured axons.

Increased levels of MBP protein in AD cortex have been reported in at least one previous study [50]. Thus, our results confirm that the levels of MBP and dMBP are increased in AD cortex compared to controls. The mechanism by which that MBP levels were higher in AD compared to control remains unclear. It is possible that MBP/myelin injury is associated with remyelination which increases total MBP in AD brain. In addition, we cannot rule out the possibility that the increase in "MBP" observed in AD brain is due to induction of Golli-MBP proteins that are normally expressed in neurons.

AβPP appears in injured axons in AD brain

Evidence for axonal injury in this study is supported by fragmented NF staining, and the co-localization of the fragmented NF staining in axons with staining for AβPP. AβPP occurs in neurons of normal adult cortex and in neurons in AD cortex [51]. Of interest, AβPP has been identified as a reliable axonal injury marker in traumatic brain injury [52–57]. Indeed, we found AβPP appeared in injured axons in AD brain but not in normal axons in control brains presumably because it accumulates at sites of axonal injury with impaired axonal transport of the AβPP.

Because of the abnormal appearance of AβPP in axons in AD brain, we examined localization of shorter peptide products. N-terminal short fragments including Aβ$_{1-16}$ and Aβ$_{17-24}$ were found in pyramidal neurons in AD brains, whereas Aβ$_{1-42}$ was not identified in pyramidal neurons of AD brains. Since the antibodies to Aβ$_{1-16}$ and Aβ$_{17-24}$ might also detect AβPP, these data are difficult to interpret. However, they might suggest that AD pyramidal neurons process AβPP/Aβ$_{1-16}$/Aβ$_{17-24}$ differently than Aβ$_{1-42}$. Alternatively, Aβ$_{1-42}$ might be rapidly cleared from neurons and not be detectable immunocyto-chemically. These findings are consistent with a substantial literature showing that Aβ peptides and AβPP can be found in neurons in AD brains with some investigators suggesting intracellular Aβ/AβPP being involved in AD pathogenesis [58].

MBP, dMBP, and Aβ$_{1-42}$ in amyloid plaques

Recent evidence has demonstrated that Aβ and especially Aβ$_{1-42}$ is generated from AβPP during autophagic turnover of AβPP-rich organelles supplied by both autophagy and endocytosis [59]. During autophagy, organelles are sequestered into auto-phago-somes that fuse with lysosomes as autophagolyso-somes where organelles are processed or degraded. Proteases in lysosomes such as cathespins can cleave AβPP to produce Aβ [59, 60] and cathespins have been identified in the amyloid plaques. Since we find the lysosomal marker LC3b associated with myelinated axons, and AβPP appears in fragmented axons in AD brain, it is possible that one source of AβPP derived Aβ$_{1-42}$ in amyloid plaques is from fragmented axons where AβPP is accumulated.

Fragmentation of myelinated axons may contribute to amyloid plaque. This idea is supported by the localization of MBP and dMBP with amyloid plaques in this study. MBP was present at the margins of amyloid

plaques whereas dMBP co-localized with $A\beta_{1-42}$ in the plaque core. The association of dMBP with $A\beta$ is consistent with recent biochemical studies [24, 33, 34]. MBP is previously identified as a novel $A\beta$ chaperone protein that binds $A\beta$ and is an inhibitor of $A\beta$ fibrillary assembly via residues 54 to 64 in MBP [24, 33, 34]. Moreover, intact purified MBP can degrade $A\beta$ protein and peptides, whereas degraded MBP lacking autolytic activity cannot degrade $A\beta_{40}$ or $A\beta_{42}$ [33]. Recently, a study in bigenic Tg-5xFAD/MBP$^{-/-}$ mice shows a significant decrease of insoluble $A\beta$ and decreased parenchymal plaque deposition at an early age [61]. These studies suggest that some form of MBP is necessary for plaque formation. Since MBP is completely knocked out in bigenic Tg-5xFAD/MBP$^{-/-}$ mice, it is hard to know whether intact MBP or degraded MBP is involved in $A\beta$ deposition in the amyloid plaques in that model.

It is notable that neither MBP nor NF co-label with FSB stained amyloid, which might mean they are both intracellular. Thus, based upon these facts and our data we postulate that intact intracellular MBP at the margins of plaques might degrade $A\beta$ and limit amyloid formation whereas extracellular degraded MBP might bind $A\beta_{1-42}$ but not degrade it, thus possibly contributing to formation of plaques.

MBP could also be involved in amyloid plaque formation via additional mechanisms. LRP1 is a major receptor for $A\beta$PP endocytosis [62] and a major efflux transporter for $A\beta$ across the blood-brain barrier [63]. LRP1 has also been found to be an essential receptor for endocytosis of degraded myelin and LRP1 directly binds intact MBP [64]. Thus, if dMBP also binds LRP1 and dMBP increases in AD brain, it would compete with $A\beta$ for transport by LRP1, which could decrease $A\beta$ clearance from the brain to blood. Finally, $A\beta$ is toxic to myelin-producing oligodendrocytes [35, 65] which could contribute to formation of additional MBP and dMBP in AD cortex. A myelin-associated enzyme, $2',3'$-Cyclic-nucleotide $3'$-phosphodiesterase (CNPase), is expressed exclusively by oligodendrocytes in the central nervous system. In the current study, the mass spectroscopy analysis shows an interaction of $A\beta_{1-42}$ with CNPase as well as MBP, which suggests that several oligodendrocyte proteins associate with amyloid plaques in AD brain.

Interaction of dMBP with $A\beta$PP and $A\beta_{1-42}$

An interaction between dMBP and $A\beta$PP is suggested by the co-immunoprecipitation experiments. Given a molecular weight of full length $A\beta$PP of 87

kDa and a molecular weight of MBP of 18–21 kDa, the $\sim$27 kDa band may be a complex of dMBP and cleaved $A\beta$PP (c$A\beta$PP). If so, the dMBP-c$A\beta$PP complex is observed in control brain, but is found at higher levels in AD brain. The c$A\beta$PP complexed with dMBP may contain the $A\beta_{1-42}$ fragment since a protein with similar molecular weight is also detected in the $A\beta_{1-42}$ IP product immunoblotted with the dMBP antibody.

In the control co-immunoprecipitation experiment using an antibody to IgG for the pull down, a $\sim$28 kDa band is detected on the $A\beta$PP immunoblot in control and AD brain but not in the PBS lane. This suggests that IgG light chain or a light chain fragment binds a cleaved fragment of $A\beta$PP resulting in a $\sim$28 kDa complex.

IgG has been detected in specific populations of cortical pyramidal neurons that appear to be degenerating in AD brains [66]. Moreover, a recent study has shown that IgG positive neurons in AD brains are dying via the classical antibody-dependent complement pathway [67]. Therefore, these data support the possibility that IgG might interact with c$A\beta$PP in addition to c$A\beta$PP interactions with dMBP in AD brains. Future studies will be needed to determine whether these interactions might mediate cell death and/or axonal and myelin injury in AD brain or are the result of cell injury.

Additional evidence for MBP interacting with $A\beta_{1-42}$ came from the MS studies. Using an antibody to $A\beta_{1-42}$ for immunoprecipitation, we find that the IP product contained MBP as well as neurofilament proteins, tau, and heat shock proteins. Indeed, the relative amounts of MBP were greater than $A\beta$PP and tau.

Limitations of the study

This study has several limitations. These findings are associations, and thus cause and effect cannot be established. Future studies will need to assess whether MBP and/or dMBP also associate with diffuse, compact, or immature senile plaques; whether the same findings apply to other brain regions including those less affected in AD brain; and whether MBP/dMBP associate with amyloid plaques early in the disease course. Indeed, since all of the brains in this study were late stage, it is not possible to state whether dMBP and MBP might participate in formation of amyloid plaques, or whether dMBP and MBP are only deposited in plaques once they are fully formed.

The data are based upon postmortem brain tissue and thus conclusions must be tempered by the possibility that some findings related to postmortem changes. However, since the postmortem intervals were similar

for the AD and control brains, it seems unlikely that the differences for dMBP, MBP, AβPP, and Aβ between AD and control brains found here were related to post-mortem changes.

Future studies should also assess whether MBP and/or dMBP associate with tau, though tau and MBP were both pulled down in the IP product with an antibody to $Aβ_{1-42}$. Though a relationship between damaged axons and myelin and amyloid plaques is shown here, details of their interactions remain unclear. It will be interesting to determine if animal AD models show an association between dMBP/MBP and amyloid plaques which appears to be the case in our preliminary unpublished studies.

ACKNOWLEDGMENTS

Authors' disclosures available online (http://www.j-alz.com/disclosures/view.php?id=2608).

SUPPLEMENTARY MATERIAL

The supplementary material is available in the electronic version of this article: http://dx.doi.org/10.3233/JAD-142013.

REFERENCES

[1] Querfurth HW, LaFerla FM (2010) Alzheimer's disease. *N Engl J Med* **362**, 329-344.

[2] Alzheimer A, Forstl H, Levy R (1991) On certain peculiar diseases of old age. *Hist Psychiatry* **2**, 71-101.

[3] Moller HJ, Graeber MB (1998) The case described by Alois Alzheimer in 1911. Historical and conceptual perspectives based on the clinical record and neurohistological sections. *Eur Arch Psychiatry Clin Neurosci* **248**, 111-122.

[4] Strittmatter WJ, Saunders AM, Schmechel D, Pericak-Vance M, Enghild J, Salvesen GS, Roses AD (1993) Apolipoprotein E: High-avidity binding to beta-amyloid and increased frequency of type 4 allele in late-onset familial Alzheimer disease. *Proc Natl Acad Sci U S A* **90**, 1977-1981.

[5] Corder EH, Saunders AM, Strittmatter WJ, Schmechel DE, Gaskell PC, Small GW, Roses AD, Haines JL, Pericak-Vance MA (1993) Gene dose of apolipoprotein E type 4 allele and the risk of Alzheimer's disease in late onset families. *Science* **261**, 921-923.

[6] Wallin A, Gottfries CG, Karlsson I, Svennerholm L (1989) Decreased myelin lipids in Alzheimer's disease and vascular dementia. *Acta Neurol Scand* **80**, 319-323.

[7] Satoi H, Tomimoto H, Ohtani R, Kitano T, Kondo T, Watanabe M, Oka N, Akiguchi I, Furuya S, Hirabayashi Y, Okazaki T (2005) Astroglial expression of ceramide in Alzheimer's disease brains: A role during neuronal apoptosis. *Neuroscience* **130**, 657-666.

[8] Mielke MM, Lyketsos CG (2010) Alterations of the sphingolipid pathway in Alzheimer's disease: New biomarkers and treatment targets? *Neuromolecular Med* **12**, 331-340.

[9] Han X, D MH, McKeel DW Jr, Kelley J, Morris JC (2002) Substantial sulfatide deficiency and ceramide elevation in very early Alzheimer's disease: Potential role in disease pathogenesis. *J Neurochem* **82**, 809-818.

[10] Bartzokis G, Cummings JL, Sultzer D, Henderson VW, Nuechterlein KH, Mintz J (2003) White matter structural integrity in healthy aging adults and patients with Alzheimer disease: A magnetic resonance imaging study. *Arch Neurol* **60**, 393-398.

[11] Bartzokis G, Sultzer D, Cummings J, Holt LE, Hance DB, Henderson VW, Mintz J (2000) *In vivo* evaluation of brain iron in Alzheimer disease using magnetic resonance imaging. *Arch Gen Psychiatry* **57**, 47-53.

[12] Bartzokis G, Sultzer D, Lu PH, Nuechterlein KH, Mintz J, Cummings JL (2004) Heterogeneous age-related breakdown of white matter structural integrity: Implications for cortical "disconnection" in aging and Alzheimer's disease. *Neurobiol Aging* **25**, 843-851.

[13] Braak H, Del Tredici K, Schultz C, Braak E (2000) Vulnerability of select neuronal types to Alzheimer's disease. *Ann N Y Acad Sci* **924**, 53-61.

[14] Chia LS, Thompson JE, Moscarello MA (1984) X-ray diffraction evidence for myelin disorder in brain from humans with Alzheimer's disease. *Biochim Biophys Acta* **775**, 308-312.

[15] de la Monte SM (1989) Quantitation of cerebral atrophy in preclinical and end-stage Alzheimer's disease. *Ann Neurol* **25**, 450-459.

[16] Englund E, Brun A, Alling C (1988) White matter changes in dementia of Alzheimer's type. Biochemical and neuropathological correlates. *Brain* **111**(Pt 6), 1425-1439.

[17] Gottfries CG, Karlsson I, Svennerholm L (1996) Membrane components separate early-onset Alzheimer's disease from senile dementia of the Alzheimer type. *Int Psychogeriatr* **8**, 365-372.

[18] Roher AE, Weiss N, Kokjohn TA, Kuo YM, Kalback W, Anthony J, Watson D, Luehrs DC, Sue L, Walker D, Emmerling M, Goux W, Beach T (2002) Increased A beta peptides and reduced cholesterol and myelin proteins characterize white matter degeneration in Alzheimer's disease. *Biochemistry* **41**, 11080-11090.

[19] Svennerholm L, Gottfries CG (1994) Membrane lipids, selectively diminished in Alzheimer brains, suggest synapse loss as a primary event in early-onset form (type I) and demyelination in late-onset form (type II). *J Neurochem* **62**, 1039-1047.

[20] Terry RD, Gonatas NK, Weiss M (1964) Ultrastructural studies in Alzheimer's presenile dementia. *Am J Pathol* **44**, 269-297.

[21] Bartzokis G (2004) Age-related myelin breakdown: A developmental model of cognitive decline and Alzheimer's disease. *Neurobiol Aging* **25**, 5-18; author reply 49-62.

[22] Braak H, Braak E (1997) Frequency of stages of Alzheimer-related lesions in different age categories. *Neurobiol Aging* **18**, 351-357.

[23] Braak H, Braak E, Kalus P (1989) Alzheimer's disease: Areal and laminar pathology in the occipital isocortex. *Acta Neuropathol* **77**, 494-506.

[24] Kotarba AE, Aucoin D, Hoos MD, Smith SO, Van Nostrand WE (2013) Fine mapping of the amyloid beta-protein binding site on myelin basic protein. *Biochemistry* **52**, 2565-2573.

[25] Mirra SS, Heyman A, McKeel D, Sumi SM, Crain BJ, Brown-lee LM, Vogel FS, Hughes JP, van Belle G, Berg L (1991) The Consortium to Establish a Registry for Alzheimer's Disease (CERAD). Part II. Standardization of the neuropathologic assessment of Alzheimer's disease. *Neurology* **41**, 479-486.

[26] Sato K, Higuchi M, Iwata N, Saido TC, Sasamoto K (2004) Fluoro-substituted and 13C-labeled styrylbenzene derivatives for detecting brain amyloid plaques. *Eur J Med Chem* **39**, 573-578.

[27] Stokin GB, Lillo C, Falzone TL, Brusch RG, Rockenstein E, Mount SL, Raman R, Davies P, Masliah E, Williams DS, Goldstein LS (2005) Axonopathy and transport deficits early in the pathogenesis of Alzheimer's disease. *Science* **307**, 1282-1288.

[28] Nesvizhskii AI, Keller A, Kolker E, Aebersold R (2003) A statistical model for identifying proteins by tandem mass spectrometry. *Anal Chem* **75**, 4646-4658.

[29] Ihara M, Polvikoski TM, Hall R, Slade JY, Perry RH, Oakley AE, Englund E, O'Brien JT, Ince PG, Kalaria RN (2010) Quantification of myelin loss in frontal lobe white matter in vascular dementia, Alzheimer's disease, and dementia with Lewy bodies. *Acta Neuropathol* **119**, 579-589.

[30] Zhan X, Ander BP, Jickling GC, Liu DZ, Stamova B, Cox C, Jin L-W, DeCarli C, Sharp FR (2014) Myelin injury and degraded myelin vesicles in Alzheimer's disease. *Curr Alzheimer Res* **11**, 232-238.

[31] Repnik U, Stoka V, Turk V, Turk B (2012) Lysosomes and lysosomal cathepsins in cell death. *Biochim Biophys Acta* **1824**, 22-33.

[32] Yamashima T (2012) Hsp70.1 and related lysosomal factors for necrotic neuronal death. *J Neurochem* **120**, 477-494.

[33] Liao MC, Ahmed M, Smith SO, Van Nostrand WE (2009) Degradation of amyloid beta protein by purified myelin basic protein. *J Biol Chem* **284**, 28917-28925.

[34] Liao MC, Hoos MD, Aucoin D, Ahmed M, Davis J, Smith SO, Van Nostrand WE (2010) N-terminal domain of myelin basic protein inhibits amyloid beta-protein fibril assembly. *J Biol Chem* **285**, 35590-35598.

[35] Desai MK, Mastrangelo MA, Ryan DA, Sudol KL, Narrow WC, Bowers WJ (2010) Early oligodendrocyte/myelin pathology in Alzheimer's disease mice constitutes a novel therapeutic target. *Am J Pathol* **177**, 1422-1435.

[36] Desai MK, Sudol KL, Janelsins MC, Mastrangelo MA, Frazer ME, Bowers WJ (2009) Triple-transgenic Alzheimer's disease mice exhibit region-specific abnormalities in brain myelination patterns prior to appearance of amyloid and tau pathology. *Glia* **57**, 54-65.

[37] Peters A, Moss MB, Sethares C (2000) Effects of aging on myelinated nerve fibers in monkey primary visual cortex. *J Comp Neurol* **419**, 364-376.

[38] Nielsen K, Peters A (2000) The effects of aging on the frequency of nerve fibers in rhesus monkey striate cortex. *Neurobiol Aging* **21**, 621-628.

[39] Brun A, Englund E (1986) A white matter disorder in dementia of the Alzheimer type: A pathoanatomical study. *Ann Neurol* **19**, 253-262.

[40] Wang DS, Bennett DA, Mufson EJ, Mattila P, Cochran E, Dickson DW (2004) Contribution of changes in ubiquitin and myelin basic protein to age-related cognitive decline. *Neurosci Res* **48**, 93-100.

[41] Renkawek K, Bosman GJ (1995) Anion exchange proteins are a component of corpora amylacea in Alzheimer disease brain. *Neuroreport* **6**, 929-932.

[42] Pernber Z, Blennow K, Bogdanovic N, Mansson JE, Blomqvist M (2012) Altered distribution of the gangliosides GM1 and GM2 in Alzheimer's disease. *Dement Geriatr Cogn Disord* **33**, 174-188.

[43] Han X (2007) Potential mechanisms contributing to sulfatide depletion at the earliest clinically recognizable stage of Alzheimer's disease: A tale of shotgun lipidomics. *J Neurochem* **103**(Suppl 1), 171-179.

[44] Ishino H, Otsuki S (1975) Distribution of Alzheimer's neurofibrillary tangles in the basal ganglia and brain stem of progressive supranuclear palsy and Alzheimer's disease. *Folia Psychiatr Neurol Jpn* **29**, 179-187.

[45] Iqbal K, Grundke-Iqbal I, Merz PA, Wisniewski HM (1982) Alzheimer Neurofibrillary tangle: Morphology and biochemistry. *Exp Brain Res Suppl* **5**, 10-14.

[46] Murphy GM Jr, Eng LF, Ellis WG, Perry G, Meissner LC, Tinklenberg JR (1990) Antigenic profile of plaques and neurofibrillary tangles in the amygdala in Down's syndrome: A comparison with Alzheimer's disease. *Brain Res* **537**, 102-108.

[47] Ball MJ, Nuttall K (1980) Neurofibrillary tangles, granulovacuolar degeneration, and neuron loss in Down Syndrome: Quantitative comparison with Alzheimer dementia. *Ann Neurol* **7**, 462-465.

[48] Thom M, Liu JY, Thompson P, Phadke R, Narkiewicz M, Martinian L, Marsdon D, Koepp M, Caboclo L, Catarino CB, Sisodiya SM (2011) Neurofibrillary tangle pathology and Braak staging in chronic epilepsy in relation to traumatic brain injury and hippocampal sclerosis: A post-mortem study. *Brain* **134**, 2969-2981.

[49] Braskie MN, Klunder AD, Hayashi KM, Protas H, Kepe V, Miller KJ, Huang SC, Barrio JR, Ercoli LM, Siddarth P, Satyamurthy N, Liu J, Toga AW, Bookheimer SY, Small GW, Thompson PM (2010) Plaque and tangle imaging and cognition in normal aging and Alzheimer's disease. *Neurobiol Aging* **31**, 1669-1678.

[50] Selkoe DJ, Brown BA, Salazar FJ, Marotta CA (1981) Myelin basic protein in Alzheimer disease neuronal fractions and mammalian neurofilament preparations. *Ann Neurol* **10**, 429-436.

[51] McGeer PL, Akiyama H, Kawamata T, Yamada T, Walker DG, Ishii T (1992) Immunohistochemical localization of beta-amyloid precursor protein sequences in Alzheimer and normal brain tissue by light and electron microscopy. *J Neurosci Res* **31**, 428-442.

[52] Bennett RE, Mac Donald CL, Brody DL (2012) Diffusion tensor imaging detects axonal injury in a mouse model of repetitive closed-skull traumatic brain injury. *Neurosci Lett* **513**, 160-165.

[53] Johnson MW, Stoll L, Rubio A, Troncoso J, Pletnikova O, Fowler DR, Li L (2011) Axonal injury in young pediatric head trauma: A comparison study of beta-amyloid precursor protein (beta-APP) immunohistochemical staining in traumatic and nontraumatic deaths. *J Forensic Sci* **56**, 1198-1205.

[54] Corrigan F, Pham CL, Vink R, Blumbergs PC, Masters CL, van den Heuvel C, Cappai R (2011) The neuroprotective domains of the amyloid precursor protein, in traumatic brain injury, are located in the two growth factor domains. *Brain Res* **1378**, 137-143.

[55] Gentleman SM, Nash MJ, Sweeting CJ, Graham DI, Roberts GW (1993) Beta-amyloid precursor protein (beta APP) as a marker for axonal injury after head injury. *Neurosci Lett* **160**, 139-144.

[56] Sherriff FE, Bridges LR, Gentleman SM, Sivaloganathan S, Wilson S (1994) Markers of axonal injury in post mortem human brain. *Acta Neuropathol* **88**, 433-439.

[57] Sherriff FE, Bridges LR, Sivaloganathan S (1994) Early detection of axonal injury after human head trauma using immunocytochemistry for beta-amyloid precursor protein. *Acta Neuropathol* **87**, 55-62.

[58] Gouras GK, Willen K, Tampellini D (2012) Critical role of intraneuronal Abeta in Alzheimer's disease: Technical challenges in studying intracellular Abeta. *Life Sci* **91**, 1153-1158.

[59] Nixon RA (2007) Autophagy, amyloidogenesis and Alzheimer disease. *J Cell Sci* **120**, 4081-4091.

[60] Cataldo AM, Paskevich PA, Kominami E, Nixon RA (1991) Lysosomal hydrolases of different classes are abnormally distributed in brains of patients with Alzheimer disease. *Proc Natl Acad Sci U S A* **88**, 10998-11002.

[61] Ou-Yang MH, Van Nostrand WE (2013) The absence of myelin basic protein promotes neuroinflammation and reduces amyloid beta-protein accumulation in Tg-5xFAD mice. *J Neuroinflammation* **10**, 134.

[62] Holtzman DM, Herz J, Bu G (2012) Apolipoprotein e and apolipoprotein e receptors: Normal biology and roles in Alzheimer disease. *Cold Spring Harb Perspect Med* **2**, a006312.

[63] Ueno M, Nakagawa T, Wu B, Onodera M, Huang CL, Kusaka T, Araki N, Sakamoto H (2010) Transporters in the brain endothelial barrier. *Curr Med Chem* **17**, 1125-1138.

[64] Gaultier A, Wu X, Le Moan N, Takimoto S, Mukandala G, Akassoglou K, Campana WM, Gonias SL (2009) Low-density lipoprotein receptor-related protein 1 is an essential receptor for myelin phagocytosis. *J Cell Sci* **122**, 1155-1162.

[65] Xu J, Chen S, Ahmed SH, Chen H, Ku G, Goldberg MP, Hsu CY (2001) Amyloid-beta peptides are cytotoxic to oligodendrocytes. *J Neurosci* **21**, RC118.

[66] D'Andrea MR (2003) Evidence linking neuronal cell death to autoimmunity in Alzheimer's disease. *Brain Res* **982**, 19-30.

[67] D'Andrea MR (2005) Evidence that immunoglobulin-positive neurons in Alzheimer's disease are dying via the classical antibody-dependent complement pathway. *Am J Alzheimers Dis Other Demen* **20**, 144-150.